Ground-Based Luminescence Measurement at Brown-Bassett Field, Texas*

Abstract

Luminescence and reflectance measurements made on Cretaceous carbonate rocks and thin soils showed significant variation over and adjacent to the Brown-Bassett gas field. Luminescence and reflectance were measured for ten rock and ten soil samples at each of 40 sites using a Fraunhofer Line Radiometer. Analysis of variance models with lithologic descriptors for color, lithology, and texture as covariates were used to calculate average values of luminescence for each site. The lithologic descriptors were assigned ordinal values based on a hierarchical scheme, then tested for significance using t-tests prior to inclusion in the model. Significant differences were observed between site means. Sites with high luminescence generally corresponded to areas overlying or near the Brown-Bassett field. Sites with low values of luminescence were generally off-field. The total range of mean values for relative luminescence of rocks and soils at the 40 measured sites was three times the average variation of luminescence of samples at a site.

Introduction

The major objectives of this study were to (1) demonstrate that solar stimulated luminescence related to alteratrion of surface rocks could be measured with a passive system and (2) provide ground-truth support for a proprietary remote sensor which was under development by ARCO. The Brown-Bassett field was chosen as a luminescence test site because of availabile proprietary subsurface information and the well-defined extent of the reservoir. The field is readily visible on both MSS and TM imagery, but the usefulness of such imagery is limited by high albedo in all bands and high band-to-band correlation. No evidence of surface alteration or spectral differences between on-field and off-field areas was detected.

The Brown-Bassett study area encompasses the Brown-Bassett gas field situated on the eastern border of Terrell County, Texas. Sun Oil Co. discovered gas in the Ordovician Ellenburger Group in 1953 in the JM field directly across the Pecos River from Brown-Bassett. Magnolia Petroleum Co. (Mobil Oil) discovered gas in both the Ellenburger and Fusselman (Silurian) formations at Brown-Bassett in 1958. The Brown-Bassett and JM fields are structurally continuous at the depth of the Ellenburger Formation (Figure 1). They are arbitrarily separated by the Terrell-Crockett County line along the Pecos River. The Brown-Bassett and JM fields are on the northeast flank of the Val Verde basin. This basin is a narrow southeast extension of the deep Delaware basin.

The combined Brown-Bassett and JM fields cover about 85 square miles. Most Ellenburger wells are drilled on a one-mile spacing and many are capable of producing more than 20 million cubic feet of gas per day. Ellenburger gas is approximately 50 percent CO_2 (Hills, 1968). In 1990, the Ellenburger Brown-Basset field produced 38.5 trillion cubic feet (TCF) of gas from 38 wells. Cumulative production for this field from 1970 through 1990 was 813 TCF of gas (Railroad Commission of Texas, 1991). About 10 TCF was produced from Silurian, Devonian, and Permian reservoirs in the 1970 to 1990 period.

The Val Verde basin contains a nearly complete Paleozoic section. The stratigraphy of the Brown-Bassett area is summarized from Webster (1980, pp. 222–225), Vertrees *et al.*(1959), Flawn et al. (1961, pp. 136–138), Calhoun and Webster (1983, pp. 101–107), Young (1960), and Hills (1968). The Ellenburger Formation (Late Cambrian to Early Ordovician) conformably overlies a thin Cambrian unit. The Ellenburger is predominantly a finely crystalline dolomite sequence that ranges from 1200 to 1600 feet thick in the Brown-Bassett area. Excellent matrix porosity (7 to 15 percent) is developed in the middle and lower parts of the Ellenburger Formation at the Brown-Basset and JM fields. Extensive fracturing and brecciation has enhanced the reservoir permeability (Vinson, 1959).

Unconformably above the Ellenburger are the Simpson Group (Ordovician), Fusselman Limestone (Silurian), an unnamed Devonian unit, the Woodford Shale (Devonian), and the Strawn formation (Pennsylvanian). More than 8,000 to 10,000 feet of Lower Permian, Wolfcamp sediments accumulated at Brown-Bassett. The Wolfcamp Group consists of poorly sorted lenticular sandstone, conglomerate, and shaley siltstone. Small amounts of gas were produced at Brown-Bassett from the Wolfcamp, but all Wolfcamp production is now abandoned or shut-in. The Wolfcamp grades upward into platform limestone, basinal shale, and argillaceous carbonates of the Leonard Formation (Lower Permian) which are

*Presented at the Ninth Thematic Conference on Geologic Remote Sensing, Pasadena, California, 8-11 February 1993.

Photogrammetric Engineering & Remote Sensing, Vol. 59, No. 8, August 1993, pp. 1257–1264.

0099-1112/93/5908–1257$03.00/0

Lester J. Walters, Jr.[1], Michael A. Wiley[2]
ARCO Oil and Gas Company, 2300 West Plano Parkway, Plano, TX 75075.

[1]Presently at PSM International, Inc., 703 McKinney Avenue, Dallas, TX 75202.

[2]Presently at The Consulting Operation, 2415 Valley View Lane, Suite 105, Farmers Branch, TX 75234.

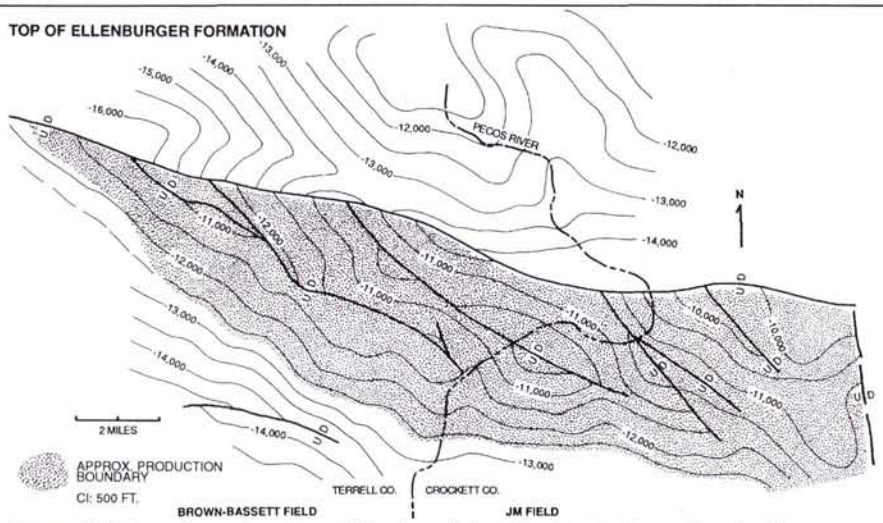

Figure 1. Subsurface structure of the top of the Ellenburger formation for Brown-Bassett and JM fields. Production in Crockett County represents the JM field; Terrell County production is assigned to the Brown-Bassett field.

the uppermost Paleozoic rocks at Brown-Bassett (Smith and Brown, 1983, p. 25).

Rocks of the Leonard Formation crop out in the Pecos River canyon at the east end of the Brown-Bassett Field. At this location, the Fort Terrett Member of the Edwards Limestone unconformably overlies the Permian rocks. The Segovia Member of the Edwards Limestone conformably overlies the Fort Terrett Member. Both of these units comprise an alternating succession of limestone and dolomite units with occasional beds of marl or marly limestone. The Lower Cretaceous section is about 450 feet thick and thickens southward. About 50 feet of Upper Cretaceous Buda Limestone overlies the Edwards Limestone. A few thin patches of the overlying Boquillas Formation, the only significant clastic unit in the field area, are preserved in the topographically higher parts of the field.

The surface of the Brown-Bassett area is a succession of broad mesas cut by steep-walled canyons. The mesas are mostly capped by resistant Cretaceous limestone on which a few centimetres of soil have developed. The canyons are 300 to 500 feet deep, narrow, and steeply inclined at their upper ends. Canyon walls are generally unstable and are being actively eroded by both mechanical and aqueous processes. Cretaceous surface rocks in the region are extensively fractured but only a few faults have been recognized (Barnes, 1981). Surface rocks are cut on the north side of the JM field by a west-northwest striking fault with 22 feet of apparent vertical displacement. Smith and Brown (1983, p. 25) claim that this is the surface expression of the major north bounding fault of both JM and Brown-Bassett fields. If their interpretation is correct, then (1) the large difference in pre- and post-Lower Cretaceous displacement demonstrates a long history of repeated faulting on this structure, (2) much of the fault displacement probably dies out in or is concealed by additional deposition in the Lower Permian rocks, (3) the fault dips about 65 degrees north, and (4) there is a possible reservoir-to-surface conduit for seepage of gas. A gas seep near the hypothetical westward extension of the surface fault was reported by ARCO geologists in 1963. The westward continuation of the surface fault in the JM field can be detected on Landsat TM imagery of the area. This can be traced approximately through the center of Brown-Bassett, passing through a disrupted, tilted outcrop of Boquillas.

Although the Crest of the Pandale surface anticline is coincident with the Brown-Bassett and JM fields, the structural trends are different. Both Brown-Bassett and JM fields are structural traps formed by a west-northwest trending fault which displaces Lower Paleozoic rocks roughly 3000 feet downward to the north. The deep structure of the Brown-Basset and JM fields shown in Figure 2 are south dipping homoclinal surfaces bounded on the north by a down-to-the-north fault with about 3000 feet displacement. Several additional down-to-the-north faults with displacements of a few hundred feet divide the fields into a succession of south dipping wedges. All of the faults are nearly vertical where they cut the Ellenburger and Fusselman reservoirs. Repeated movement along the major fault along the north side of the field is reflected by variation in thickness of Permian Wolfcamp and Leonard formations.

Repeated downwarp and uplift along a relatively narrow hinge line suggest that vertical migration of gas to the surface has been possible. However, the present subsurface interpretations of the deeper reservoirs (Figure 1) invoke the mapped faults as the updip closure mechanism for gas entrapment. The relatively high (3000 to 4000 psi) pressures and large reserves encountered in these reservoirs suggest that neither the trapping mechanism nor the overlying section is leaking excessively. The best working hypothesis seems to be a leakage pattern that has changed with time and that is probably skewed toward the north bounding fault. Abundant secondary calcite observed in the Buda could be produced by normal diagenesis or changes in the carbonate chemical equilibria caused by seepage of gas from the Ellenburger and subsequent oxidation of methane to form carbon dioxide.

Luminescence Field Program

The Brown-Bassett field was chosen as a luminescence test site because of availability of proprietary subsurface information. Usefulness of MSS and TM imagery available for the area is limited by high albedo in all bands and high band-to-band correlation. A false-color composite image constructed from the first three principal components from TM and a color ra-

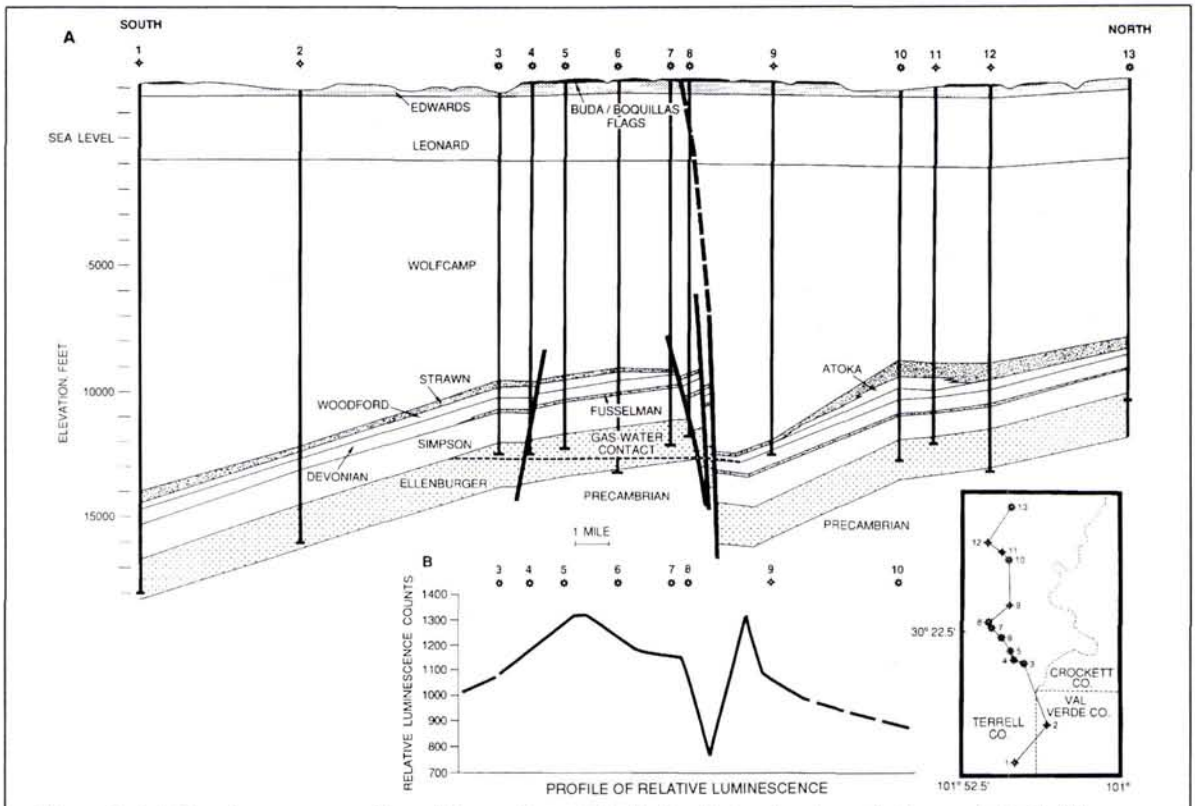

Figure 2. (a) Structure cross section of Brown-Bassett field showing major down to the north fault. (b) profile of relative luminescence along the line of cross section.

tio composite image of TM bands 4/2, 5/1, and 3/2, coded red, green, and blue, respectively, aided in mapping the Buda Limestone and Boquillas Formation.

Luminescence measurements at Brown-Bassett were made using Fraunhofer Line Radiometers (FLR) developed by Zupanic and McBride (1987) and Zupanic and Braun (1987) configured to measure light intensity at the 589.0 nm Fraunhofer line. The FLR is a passive instrument modeled after the Fraunhofer Line Discriminator developed by Perkin-Elmer Corporation (Plascyk, 1975) and the USGS (Watson and Hemphill, 1976). Although higher signal-to-noise ratios could be obtained through the use of an active system based on luminescence stimulation with a light source, the use of a passive system was required because of the association with the proprietary remote sensor developed by ARCO.

The 589.0-nm Fraunhofer line and associated line at 589.6 nm are narrow bands of low intensity in the solar radiation spectrum (Figure 3) resulting from absorption of light by sodium vapor in a cool region surrounding the sun. The FLR instruments measure the relative light intensity within the Fraunhofer line (Figure 3c) as compared to the light intensity adjacent to the line (Figure 3b). Reflected light corresponds to the relative intensity of the solar spectrum whereas light produced by luminescence in carbonate minerals has a maximum intensity at approximately 615 nm (Marfunin, 1979). Significant induced luminescence, present at this wavelength, results in an increase in the ratio of light energy in the narrow Fraunhofer wavelength band to the light energy in the surrounding wavelength region.

Luminescence measurements using the FLR instruments were made on samples of rocks and soil, within a 200 by 200 foot area (1 acre) at each site. Ten slabs of rock that seemed typical of the area were gathered, numbered, described, and photographed. The slabs were then moved under the instrument and read without moving the instrument. After measurement, a small sample of each slab was collected for future laboratory study. Ten soil exposures (tripod stations) were selected randomly at each site. These exposures were generally 20 to 30 feet apart in roughly circular pattern, and the FLR was moved from one to another. All measurements for a site could be completed wihin one to 1.5 hours under optimum conditions.

Four reflectance and four luminescence standards were routinely measured at each site. Reflectance calibration plates with a near-Lambertian surface (Zupanic, 1991) ranged from about 85 percent to 8 percent reflectance at 589 nm. Luminescence plates containing a fluorescent rhodamine dye dissolved in acrylic plastic were also measured. One luminescence plate was used unmodified (the 100 percent plate). The other three plates were modified by laying a 10 percent, 30 percent, and 50 percent drafting screen over the plate surface to produce 90 percent, 70 percent, and 50 percent luminescence values. Measurements of one or more of the reflectance plates were repeated at each tripod location. All of the luminescence standards were measured at the first and last tripod location at each site.

The internal temperature of the radiometer's optical components, which was recorded automatically, was used to represent the temperature of the luminescence plates. Correction was made for variation in luminescence response with temperature using the data of Watson (1975) for rhodamine-WT dye in water. Watson's data for rhodamine-WT solutions

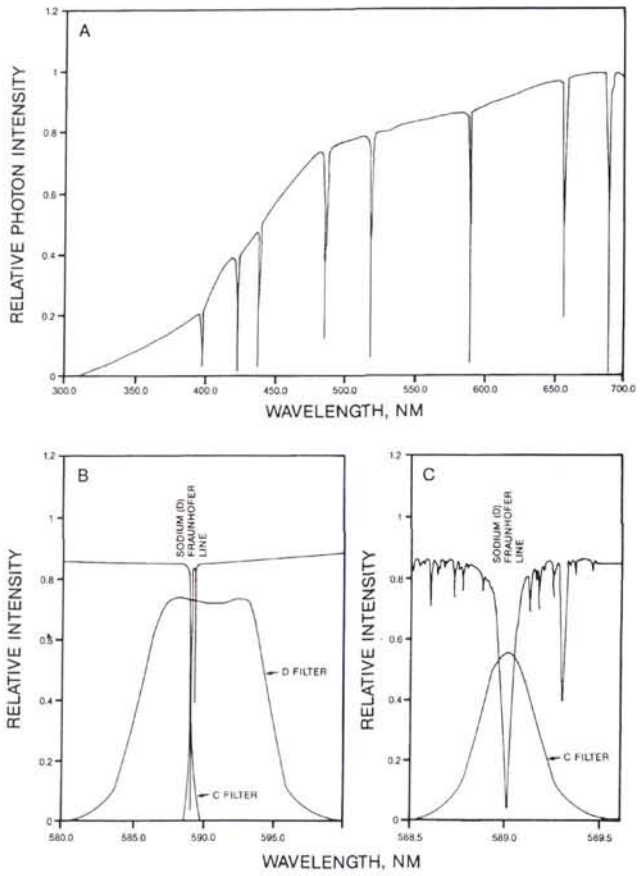

Figure 3. (a) Solar spectrum showing Fraunhofer lines, (b) relation between the sodium (D) Fraunhofer line and the D and C channel filters, (c) detail solar spectrum showing the Sodium (D) Fraunhofer line, C channel filter, and numerous absorption bands due to water vapor. Spectral data were obtained from the Kit Peak Observatory.

showed that luminescence decreased 50 percent over the temperature range 20 to 50 degrees Celsius. Subsequent research by Walters at ARCO showed that the amount of luminescence emitted by the orange plastic plates decreased approximately 10 percent over the range 8.8 to 60.7 degrees Celsius. The temperature range observed during luminescence measurements was 36 to 53 degrees Celsius. Thus, the Brown-Bassett data were apparently over-corrected based on the more recent work. The excessive temperature correction caused a decrease in the apparent luminescence calculated but does not eliminate any anomalous values in the study.

Data were collected only while the sun elevation angle exceeded 40 degrees. In July, at Brown-Bassett, this was approximately 9:50 AM CDT to 5:50 PM CDT. Clouds ranging from thin, high cirrus to cumulus and low stratus were encountered on about 60 percent of the days worked. The cirrus clouds were not generally a problem, but attempts to "shoot through holes" in the cumulus and stratus clouds yielded data of lower to very poor quality.

The data reduction process for data from the FLR's consisted of the following steps: (1) field data collected in the TRS-80 Model 100 computers were transfered to a portable computer each night in the form of disk files; (2) the disk files were transfered to ARCO's host computer; (3) SAS-compatible files (SAS Institute, Inc., 1985) were created from the raw data files; (4) extensive examination of the data for all reflectance plates and luminescence plates was performed during the data screening step; and (5) reflectance and luminescence were calculated for all rocks and soils based on calibration curves from the reflectance and luminescence plates.

The data collection and control program in the TRS-80 Model 100 computer, which is directly linked to the FLR controls instrument operation, records the field data, and provides data quality control information to the operator. Each measurement channel is read eight times to produce a line of data containing average values for all channels. This process is automatically repeated ten times for all measurements. The mean, standard deviation, and coefficient of variation (CV) of each instrument channel were then computed. If the CV of the ten readings in all of the three instrument channels was less than 0.5 percent, the mean, standard deviation, and CV for the sample are read into permanent memory and the operator is prompted to continue to the next sample or standard. However, if the CV of any channel exceeds the preset value, a second and, if needed, a third attempt to obtain data was initiated automatically by the computer program.

The data were read into the ARCO mainframe computer for reformatting and editing. A suite of SAS (SAS Institute Inc., 1985) computer programs was used to apply scaling factors and correct for measured detector dark current, temperature, calculated sun elevation angle, and ambient light intensity. The programs also produced plots of each channel for the reflectance plates. All readings identified by this process were scrutinized to determine probable causes for any apparently bad data. Data acquired over natural surfaces and reference standards were both screened in this step.

Luminescence of the orange plastic standards was related to solutions of rhodamine-WT in concentration units of parts per billion. Subsequent determination of the absolute luminescence coefficient of these plastics indicates that the relative luminescence values in this report can be converted to absolute luminescence coefficients by dividing by 22000. The conclusions of this report are not scale dependent; therefore, relative luminescence units related to ppb rhodamine-WT will be retained. Reflectance was calculated as the ratio of reflected light intensity to incident light intensity using the standard reflectance plates.

Tests were conducted throughout the processing to assure statistical significance of the final luminescence and reflectance values. No significant differences (95 percent confidence level) were found between the two instruments used for measurement, or between rocks and soils. Hence, the data from both instruments were combined. Data for rocks and soils at each site were also combined to calculate a mean value response for the site.

Calculation of Luminsecence and Reflectance

The observed signals for the C and D channels (Figure 3) were corrected for dark currents and normalized to a standard illumination of 1000 watts/m² based on the response of an alphatometer which measured the total solar intensity over a broad spectral range to give

$$CXX = (Cobs - F) * \alpha/(E - Eo) \quad (1)$$

$$DXX = (Dobs - G) * \alpha/(E - Eo) \quad (2)$$

where CXX and DXX are analogous to normalized c and d for the FLD (Plascyk, 1975; Watson and Hemphill, 1976); F, G,

and Eo are dark currents; α is the responsivity of the alphatometer; and E is the alphatometer signal. Laboratory calibration of the instruments indicated that the dark currents F and G as well as a were best represented by instrument specific first- or second-order functions of the temperature of the FLR electronics which was one of the output data channels. The value used for determination of Eo was the average value for a "glob" of data (80 readings) collected at each site with the lens cap on the alphatometer. Calibration studies also indicated that the alphatometer responsivity (a) was an instrument specific function of temperature. Two additional parameters are needed to calculate reflectance (R) and luminescence (L) from the above signals. The first is Kt which is the ratio of the electro-optical gains of the C and D channels and is determined by observing a quartz-halogen lamp which does not contain the Fraunhofer line in its output spectrum. Measurement of Kt is made in the laboratory for each FLR. The second parameter is Ko which is the ratio of the D and C channels (corrected for dark current) using sunlight reflected from a target with no luminescence. Reflectance and luminescence are calculated from CXX, DXX, Ko, and Kt using

$$\text{RCOUNT} = (\text{DXX} - \text{Kt} * \text{CXX})/(\text{Ko} - \text{Kt}) \quad (3)$$

$$\text{LCOUNT} = (\text{Ko} * \text{CXX} - \text{DXX})(\text{Ko} - \text{Kt}) \quad (4)$$

where RCOUNT and LCOUNT are proportional to the absolute reflectance and luminescence coefficients. The parameter Ko was determined for each day, site, and FLR combination using the data for reflectance plates. These plates have very low luminescence, which was assumed to be zero. Thus, Equation 4 can be solved for Ko. Plots of DXX/CXX versus time, solar zenith angle, secant-corrected alphatometer response, FLR temperature and reflectance for all readings of reflectance plates, suggested that Ko was not a constant. Minor dependence on other parameters suggested that Ko should have a more complex form to better fit the data for each day, site, and FLR combination. Stepwise linear regression using procedure STEPWISE (SAS Institute, 1985) was used to determine the coefficients A1 to A4 for the model

$$\text{Ko} = \text{Constant} + \text{A1} * \text{Z} + \text{A2} * \text{Cos(Z)} + \text{A3} * (\text{Tb} - 30) + \text{A4} * (\text{E} - \text{Eo}) * \text{Sec(Z)} \quad (5)$$

where Z is the solar zenith angle in degrees. The solar zenith angle (Z) at the time of each measurement was calculated based on the Julian date, latitude, longitude, and local time. The values of the reflectance plates were corrected for deviation from Lambertian response using a function of the zenith angle and calibration data of P. Slater (personal communication, 1985).

Interpretation of FLR Data

Measurements of luminescence and reflectance at 589 nm of 410 rock samples and 413 soil samples were made at 40 sites, each having an area of about an acre. During final data screening, measurements of 44 rock samples and 45 soil samples were discarded because of statistically determined erratic departure from the mean value of luminescence of rocks or soils at each site.

The vertical projection to the surface of the gas-water contact in the underlying Ellenburger reservoir, the major fault on the north side of the field, and the location of producing wells were used to classify sites into *on-field* and *off-field* categories. Designation of on-field and off-field areas was based on the presence or absence of petroleum production, an economic rather than a physical property. Therefore, well records and logs of dry holes were examined for suggestions of significant shows or potential production. A subjective reclassification of all sites was then made based on proximity to wells with moderate to strong gas shows. After reclassification, 20 sites were designated *on-field*, 14 sites were designated *off-field*, and six sites within 0.6 miles of a well with shows were designated *show*.

The ANOVA with the three classes indicates no significant difference between the three classes for luminescence of rocks or soils. The reflectance of on-field rocks (0.393) is significantly brighter than the reflectance of off-field rocks (0.338). No significant difference was observed for the reflectance of soils. Interpretation of the reflectance values suggests that on-field rocks contain more secondary calcite cement, which is highly reflective, than off-field rocks. No difference would be expected in soils developed on-field or off-field because both areas are carbonate terrain. The total range of luminescence values is 525 units, with both the lowest and highest values occurring at off-field locations. The scatter in the data is about 25 percent of the total range and is one reason that ANOVA indicated no significant differences. Part of this scatter is caused by noise and inaccuracy inherent in the measurement process, but part is also caused by differences in mineralogy, surface texture, and surface coatings of the rocks and soils sampled.

A brief description and color photograph was obtained for all rock samples and most soils samples. Descriptions were limited to color, grain size, lithology, surface texture, secondary calcite, inclusions, and surface coatings. There was no obvious visual difference between on-field and off-field rock and soil samples at any of the 37 sites on the Buda Limestone with respect to these parameters. Although somewhat different from the Buda rocks and soils, the Two Edwards Limestone sites, one *on-field* and one *off-field*, seemed nearly identical as well. Only one *off-field* site was measured on the Boquillas Formation.

Parameters for each sample were entered into a database according to a set of *ad hoc* rules. Both the field notes and the color slides were used in this process. Each of the lithologic attributes were replaced by a number (weighting factor) according to their hierarchical scheme. Color, primary lithology, and secondary calcite attributes were assigned a value of one if present. Attributes of primary textures were assigned a value of four if present, secondary textures were assigned values of three if present, and inclusions were assigned a value of two if present. All attributes were assigned values of zero if not present. All rocks and soils had at least one category of color, primary lithology, and primary texture. Attributes of lichen cover were weighted according to the percent of the three-inch diameter measurement area covered by each color of lichen. Each color represents a different species of crustose lichen. The occurence of lichen on the rock samples varied from small specks covering 10 to 20 percent of the surface to large irregular patches covering up to 40 percent of the surface.

Mean values of relative luminescence and reflectance of rock and soil from 40 sites were calculated using the SAS general linear models procedure (SAS Institute, 1985). The model used related the observed luminescence or reflectance for each rock or soil sample at a site to a mean value for the site and the sum of lithologic covariates in the sample (Table 1). Unique mean values for relative luminescence and reflectance were calculated for each site. However, the coefficients for the covariate effects of color, lithology, and texture were based on all samples. The ANOVA (Table 1) indicated that both rocks and soils had significantly different responses for luminescence and reflectance between sites. The range of

TABLE 1. ANOVA MODELS OF LUMINESCENCE AND REFLECTANCE.

Parameter	Significant Differences Between Sites	Least Significant Difference Between Site Means	Significant Covariate Parameters	
			Increasing Effect	Decreasing Effect
Rock Luminescence	Yes	155	Cracks Nodular Ls Dk Gray Black Lichen Gray Lichen	Caliche
Soil Luminescence	Yes	149	No Covariates	
Rock Reflectance	Yes	0.095	Weathered Surface Caliche White Linen	Hackley Surface Nodular Ls Fine Gr. Ls Micritic Ls Dk Gray Dk Tan Gray Dk Gray Tan Gray Lichen
Soil Reflectance	Yes	0.046		Lt Tan Gray

mean luminescence values for rocks (640 to 1360 counts) and soils (860 to 1380) at the 40 measured sites is three times the least significant difference (150) between means determined by the ANOVA model. The range of mean reflectance for rocks (0.281 to 0.452) and soils (0.205 to 0.351) at the 40 measured sites is 1.8 times the least significant difference for rock means and 3.1 times the least significant difference for soil means. These tests were useful and informative for two reasons: (1) they showed that there were significant observable differences between rock and soil characteristics between the sites; and (2) several of the surface characteristics of the rock samples are correlated with luminescence. Variation of reflectance with rock and soil characteristics is intuitive, but variation of luminescence with such characteristics is not.

Most of the carbonate rocks at Brown-Bassett have a hard, thin rind or coating on their surface. This rind is about two millimetres thick and has a somewhat lighter color than the rest of the sample. Under broad-band ultraviolet light, most of the rinds fluoresce orange-red but some show green or blue. These colors are generally outside the 589-nm Fraunhofer line but probably cover the 656-nm line. Analysis of several Brown-Bassett rocks in the laboratory has shown that solar stimulated luminescence is most intense in the vicinity of 589 nm. These ubiquitous rinds may locally diminish rock luminescence, but they will not conceal it.

A contour map of relative luminescence at the Brown-Bassett field area is shown in Figure 4. Luminescence values are proportional to rhodamine-WT dye concentration in parts per billion. Figure 4 was hand contoured using linear interpolation between adjacent data points. Several contours are supported by single points, but all seem reasonable in the context of the general trend of the surrounding data. The standard error of the mean for all usable measurements at each site is generally less than 40 luminescence counts. The least significant difference between site means from the analysis of variance tests (Table 1) is 155 counts for rocks and 149 counts for soils. This indicates that sites whose luminescence site mean is more than about 150 counts different from the site mean of another site probably have different luminescence properties.

A large area of high relative luminescence values occurs over the central part of the Brown-Bassett field (Figure 4). Neither the east part of the field nor the contiguous JM field east of the Pecos River were sampled. As expected, a trend toward lower values occurs south of Brown-Basset. Correlation between the reservoir and luminescence is less obvious west and north of the field. The small areas of low and high relative luminescence near the north boundary of the field roughly coincide with the supposed surface location of the north bounding fault and could be explained by fractures providing complex gas seepage pathways to the surface.

The lobe of scattered high values that extends into the northwest part of the map cannot be readily explained by such fractures. This lobe more nearly coincides with the crest and northwest plunging nose of the Pandale surface anticline than the more westerly trend of the north bounding fault. The north-south area of low luminescence values near the west end of the field straddles the Ellenburger gas-water contact but seems to have no geologic explanation. However, several strong north-south Landsat lineaments pass through the low. These lineaments possibly represent a complex surface and subsurface fracture pattern that could divert and distort gas seepage patterns. Wells at the extreme north end of this low produce from Ellenburger and younger rocks. No wells have been drilled in the south part of the low.

The boundaries of Ellenburger production at Brown-Bassett are shown on Figures 1 and 4. The boundaries of Fusselman production are similar except that the formation pinches out near the Pecos River, whereas Ellenburger production continues eastward into the JM field. The southern boundary of Ellenburger production is the gas-water contact which occurs at about −12,600 feet throughout both the Brown-Bassett and JM fields. Fusselman production is limited on the south by pinchout of the formation which is roughly coincident with the underlying Ellenburger gas-water contact. The north boundary for both Ellenburger and Fusselman production is the large fault that is down thrown about 3000 feet to the north. These boundaries are well established by subsurface geology and seismic interpretation and may be used with confidence in comparing production to luminescence.

The production limits of formations younger than the Fusselman are not known with as much certainty. Six widely scattered Brown-Bassett field wells and at least one well north of the field also produce gas from the Devonian. Most of the field wells could produce Devonian gas but are not economic. The area of possible gas leakage from the Devonian reservoir is approximately the same as for the Ellenbur-

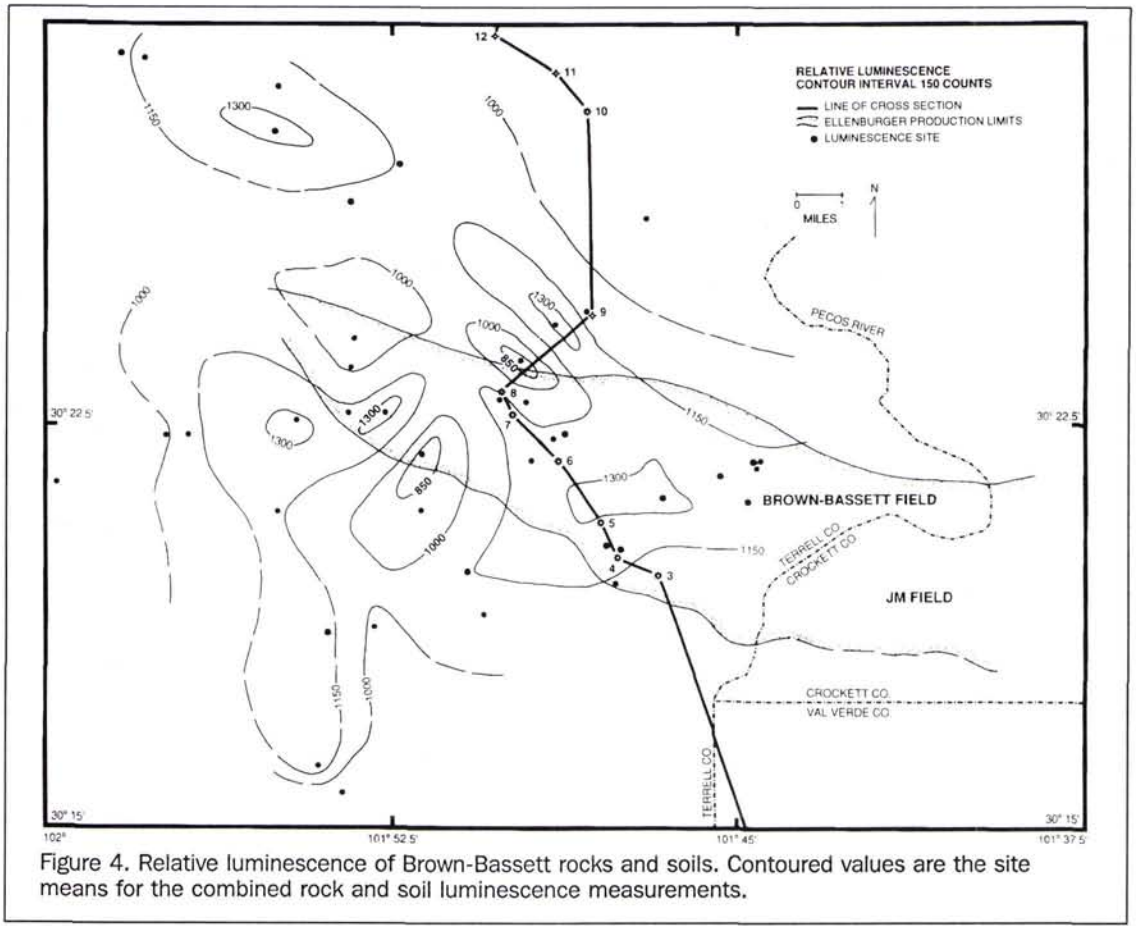

Figure 4. Relative luminescence of Brown-Bassett rocks and soils. Contoured values are the site means for the combined rock and soil luminescence measurements.

ger Formation. Several wells produce from the Strawn Formation in the eastern part of the Brown-Bassett and the western part of the JM fields. Surface alteration associated with leakage from the Strawn Formation could occur over very wide areas. Wolfcamp Group production in the region is mostly from stratigraphic or combination traps distributed over a wide area. Gas has been produced from the Wolfcamp in many wells in the Brown-Bassett and JM fields as well as from several wells to the north.

The discussion above illustrates and emphasizes one of the chief limitations of surface geochemical techniques, namely, that surface trends cannot be directly projected into the subsurface. It also shows that microseepage-induced luminescence of surface rocks can be widespread. Hence, the presence of high values over nonproducing areas should not necessarily be interpreted as erroneous indications of economic hydrocarbons at depth.

Conclusions

Significant variation in luminescence at the 589-nm Fraunhofer line was observed in and around the Brown-Basset field. The trend of the luminescence maximum generally correlates with the surface trace of the bounding fault on the north side of the field.

The Brown-Bassett area contains several *stacked* gas reservoirs, any or all of which may be leaking. The present data cannot be used to develop conclusive cause-and-effect relations between surface luminescence and subsurface gas distribution.

ANOVA tests at the 95 percent confidence level showed that lithologic descriptors such as color, texture, secondary calcite, and inclusions are significantly different between rock and soil exposures located on-field and off-field. Such differences were not obvious during collection of the lithologic data.

Ubiquitous inorganic surface coatings or rinds, probably caused by weathering, and organic coatings such as lichen, appear to affect luminescence observed at 589 nm. Relative differences remain between rocks exposed at different sample sites.

The 589-nm FLR is a usable field instrument that will, when used carefully, produce reliable luminescence and reflectance data at an acceptable rate. Reliability and efficiency can be improved by using the current advances in computer technology. The TRS-80 Model 100 was the only battery-operated portable computer available when this project was initiated.

A major improvement is possible by converting the instrument to an active system through the utilization of a UV light source and control of solar radiation. Alternatively, continuation of the luminescence research utilizing additional Franunhofer lines and a passive system would evaluate the potential for detecting petroleum and compounds with environmental importance. Success with such low-cost

ground-based systems is needed before further development of airborne systems is justified.

References

Barnes, V. E. (Project Director), 1981. *Geologic Atlas of Texas, Sonora Sheet*: University of Texas, Bureau of Economic Geology, Austin, Texas.

Calhoun, G. G., and R. E. Webster, 1983. Surface and subsurface expression of the Devils River uplift, Kinney and Val Verde Counties, Texas, *Structure and Stratigraphy of the Val Verde Basin-Devils River Uplift, Texas, Field Trip Guidebook*: (E. C. Kettenbrink, Jr., editor), West Texas Geological Society, Midland, Texas, Pub. 83-77, pp. 101-118.

Flawn, P. T., A. Goldstein Jr., P. B. King, and C. E. Weaver, 1961. The Ouachita System: Texas University, Austin, Texas, Pub. 6120, 401 p.

Hills, J. M., 1968. Gas in Delaware and Val Verde basins, west Texas and southeastern New Mexico, *Natural Gases of North America*, American Association of Petroleum Geologists Memoir 9, Vol. 2, pp. 1394–1432.

Marfunin, A. S., 1979. *Spectroscopy, Luminescence and Radiation Centers in Minerals*. Springer-Verlag, New York, 352 p.

Plascyk, J. A., 1975. The MK II Fraunhofer Line discriminator (FLD-II) for airborne and orbital remote sensing of solar-stimulated luminescence, *Optical Engineering*, Vol. 14, pp. 339–346.

SAS Institute Inc., 1985. *SAS Users Guide: Statistics, Version 5 Edition*: SAS Institute Inc., Cary, North Carolina, 956 p.

Smith, C. I., and J. B. Brown, 1983. First day road log, *Structure and Stratigraphy of the Val Verde Basin-Devils River Uplift, Texas, Field Trip Guidebook*: (Kettenbrink, E.C., Jr., editor), West Texas Geological Society, Midland, Texas, Pub. 83–77, pp. 6–26.

Railroad Commission of Texas, 1991. *Oil and Gas Division Annual Report 1990, Volume 2*: Oil and Gas Division, Railroad Commission of Texas, Austin, Texas, 344 p.

Vertrees, C., C. H. Atchison, and G. L. Evans, 1959. Paleozoic geology of the Delaware and Val Verde basins, *Geology of the Val Verde Basin and Field Trip Guidebook*: West Texas Geological Society, Midland, Texas, Pub. 59–43, pp. 54–56, map in pocket.

Vinson, M. C., 1959. Brown-Bassett field, Terrell County, *Geology of the Val Verde Basin and Field Trip Guidebook*: West Texas Geological Society, Midland, Texas, Pub. 59–43, 85 p.

Watson, R. D., 1975. Luminescence intensity of rhodamine-WT dye (5.0 ppb) as a function of temperature, *Manual of Remote Sensing, First Edition* (R. G. Reeves, editor), American Society of Photogrammetry, Falls Church, Virginia, Vol. 1, pp. 124.

Watson, R. D., and W. R. Hemphill, 1976. *Use of an Airborne Fraunhofer Line Discriminator for the Detection of Solar Stimulated Luminescence*. U.S. Geological Survey, Open File Report 76–202, 110 p.

Webster, R. E., 1980. Structural analysis of Devils River uplift southern Val Verde basin, southwest Texas: *American Association of Petroleum Geologists Bulletin*, Vol. 64, pp. 221–241.

Young, A., 1960. *Paleozoic History of the Fort Stockton-Del Rio Region, West Texas*: University of Texas, Austin, Texas, Pub. 6017, pp. 87-109.

Zupanick, J. E., 1991. *Method for Making a Reflectance Calibration Plate Having a Near-Lambertian Surface*: United States Patent 4,995,198, February 26, 1991, 2 p.

Zupanick, J. E., and C. Braun, 1987. *Temperature Compensation Means for a Radiometer*: United States Patent 4,687,335, August 18, 1987, 2 p.

Zupanick, J. E., and C. D. McBride, 1987. *Luminescence and Reflectance Detection Radiometer with Changeable Optical Assembly*: United States Patent 4,671,662, June 9, 1987, 4 p.